

## MINERAL CONTAMINANTS OF THE SEDIMENTARY KAOLIN ORE FROM IPIXUNA MINE, BRAZIL

Sydney Sabedot<sup>1</sup>

Carlos Otávio Petter<sup>2</sup>

Carlos Hoffmann Sampaio<sup>3</sup>

### ABSTRACT

The sedimentary kaolin ore of the Ipixuna Mine, in the Brazilian Amazon, contains mineral contaminants such as anatase, hematite and goethite, among others, which change the original white color of kaolin blocks to red, yellow, gray and purple. The main objective of the present study was to identify the mineral contaminants in the ROM kaolin, the textures and their relationships with the deposition environment. Binocular stereomicroscopy and X-ray diffraction were used to define the paragenesis of contaminants from different places of the ore, as well as to characterize the deposition conditions. The contaminants change the white color of kaolin ore to red, yellow, gray and purple. Red is associated with disseminated goethite and hematite in the kaolin ore. Yellow is associated with disseminated quartz, muscovite and anatase in the kaolin ore. Gray results from thin kaolinite multilayers containing low and high concentrations of anatase. Purple results from the disseminated hematite in the kaolin ore.

**Keywords:** Fe-Ti Contaminants; Kaolin ore Contaminants; Sedimentary Kaolin.

### RESUMO

**Minerais contaminantes do minério de caulim sedimentar da Mina Ipixuna, Brasil.** O minério de caulim sedimentar da mina Ipixuna, na Amazônia brasileira, contém minerais contaminantes, tais como anatósio, hematita e goetita, entre outros, cujas ocorrências alteram a cor branca original de blocos de caulim para vermelha, cinza e roxa. O principal objetivo do presente estudo foi identificar os minerais contaminantes do minério ROM de caulim, as texturas e suas relações com o ambiente de deposição. Análises por estereomicroscopia binocular e difração de raios-x permitiram definir a paragénesese mineral dos contaminantes em diversas áreas do corpo de minério, bem como caracterizar as condições de deposição. Os minerais contaminantes alteram a cor branca do minério para vermelha, amarela, cinza e roxa. A cor vermelha é associada com goetita e hematita disseminada no minério de caulim. A cor amarela é associada com quartzo, muscovita e anatósio disseminados no minério de caulim. A cor cinza é associada com finas multicamadas de caulinita contendo baixas e altas concentrações de anatósio. A cor roxa resulta da disseminação de hematita no minério de caulim.

**Palavras-chave:** Contaminantes de Fe-Ti; Minerais Contaminantes de Caulim; Caulim Sedimentar.

<sup>1</sup> PPG em Avaliação de Impactos Ambientais, Universidade La Salle – Unilasalle, Canoas, RS, Brasil. E-mail para correspondência: [sydney.sabedot@unilasalle.edu.br](mailto:sydney.sabedot@unilasalle.edu.br)

<sup>2</sup> Depto. de Engenharia de Minas, Universidade Federal do Rio Grande do Sul – UFRGS, Porto Alegre, RS, Brasil.

<sup>3</sup> Depto. de Metalurgia, Universidade Federal do Rio Grande do Sul – UFRGS, Porto Alegre, RS, Brasil.

---

## INTRODUCTION

In the Brazilian Amazon large deposits of sedimentary kaolin were formed (Murray, 2000; Sena et al., 2011). The Ipixuna Mine is the place where the present study was carried out. This mine is located in the State of Pará and its ore constitutes one of the most important Brazilian reserves of sedimentary kaolin. This reserve is part of the region known as Rio Capim. The geographical coordinates of the study area are 02° 23' S and 47° 45' W.

Many previous studies have been focused on the genesis and the age of the kaolin from the Amazon region. The Rio Jari deposit, in the State of Amapá, contains fluvial-lacustrine sediments from the Pleistocene to Holocene (Wilson et al., 1998). Deposits from Rio Capim and their chemical analysis indicated intense lateritic processes, characterized by ferruginization and deferruginization, that created the several facies (Souza et al., 2006). Studies involving heavy minerals from the Rio Capim area indicated that the age of the kaolin deposits from Ipixuna Formation is Late Cretaceous (Góes et al., 2007). Rio Jari and Rio Capim are areas where sedimentary kaolin deposits are mined and their ages are, respectively, Pliocene and Tertiary (Murray et al., 1982; Murray et al., 2007).

Many studies have been developed on the mineralogy of the Amazon kaolin deposits. The Amazon kaolin deposits were formed by well-crystallized kaolinite, quartz, illite, muscovite, hematite and anatase (Costa et al., 1998). The Rio Jari deposits have a sedimentary profile in which kaolinite is associated with gibbsite and small amounts of quartz, anatase, goethite and hematite (Montes et al., 2002). The Morro do Felipe deposit is located in the State of Amapá and their ore has hematite, goethite and anatase (Kotschoubey et al., 1999). These researchers also found sand layers with blue, purple, red and yellow colors, but they did not associate these colors to the mineral contaminants. Occurrences of high levels of  $\text{Fe}_2\text{O}_3$  (10.4%) in sedimentary kaolin layers from Rio Capim are related to the presence of hematite, goethite and anatase in the sediment layers (Carneiro et al., 2003). The same researchers show controversies particularly about the genesis of kaolin minerals in the Brazilian Amazon (Costa et al., 1998; Wilson et al., 2006). Gonçalves et al. (2007) developed a spectrophotometry technique for determining the concentration of kaolin mineral contaminants based on the Kubelka-Munk theory. Schulz Jr. (2000) and Murray et al. (2007) developed studies involving the mining and mineral processing of kaolin from the Amazon region.

The mineral paragenesis and the amount of mineral contaminants affect both mining operations and kaolin ore processing (Raghavan, 2010; Raitani et al., 2012). Brightness and yellowness values determine which ore blocks can be processed to produce the raw material with quality adequate for use in the paper industry (Bloodworth et al., 1993; Varela et al., 2005; Yanik, 2011). Ore blocks with high brightness have been scarce in the deposit. As extraction processes progress, it is necessary to extract ore blocks with higher levels of mineral contaminants, which must be removed in the mineral processing. In this context, it is important to identify the mineral contaminants and their concentrations in the ore blocks, because this information will provide technical support for mineral processing operations (Styriaková et al., 2000; Ribeiro et al., 2003; González et al., 2006). When the ore block is considered suitable for producing a final high quality raw material, in its processing it is necessary to determine a dosage of chemical for the bleaching of kaolin, as well as a time for the chemical reactions to be effective. Ore blocks with high levels of mineral contaminants are not processed because the operations to remove these minerals are not effective.

Research carried out by Sabedot et al. (2011) indicated that the Ipixuna Mine deposit is formed by run-of-mine (ROM) material blocks with low brightness (59.4%) and high yellowness (15.5%) because of high levels of  $\text{Fe}_2\text{O}_3$  and  $\text{TiO}_2$ . However, after magnetic separation and chemical bleaching processes, some ROM blocks produced a final raw material with values of 87.4% for brightness and 6.8% for yellowness. On the other hand, some ROM blocks with similar initial brightness and yellowness values (73.4% and 16.4%) that also had high levels of  $\text{Fe}_2\text{O}_3$  and  $\text{TiO}_2$  resulted in a lower quality product. These blocks were subjected to the same mineral processes and chemical dosages, but the final raw material had values of 80.3% for brightness and 13.0% for yellowness. In this case, the performance of the mineral processing was completely different for apparently similar ROM blocks, indicating that the variety of the mineral contaminant affects the effectiveness of mineral processing. Thus, it is important to identify the paragenesis of the contaminants mineral, in addition to their contents, to define if a ROM block is suitable for processing and to generate high quality raw material.

The objective of the present study was to identify the paragenesis of the mineral contaminants in ROM kaolin from the Ipixuna Mine, the associated textures and their relationships with the deposition environment. The authors examined the color of the ore, which can be associated with both the paragenesis and the concentration of contaminants. The results are expected to improve ore extraction operations, maximize financial gains, minimize the use of chemicals in bleaching operations, and minimize the environmental impacts of mining. The authors believe that the results of the present study may also contribute to the sustainable development of mining.

## MATERIALS AND METHODS

The Ipixuna deposit consists of five varieties of ROM kaolin, two of which are considered unprofitable to be benefited and three are considered profitable to be benefited to generate high quality raw material. The orebody is extracted from several areas at the same time. In this way, samples for this study could be collected at different locations. Samples were collected specifically in places where there had been lenses with high concentrations of mineral contaminants (Figure 1). Lenses with contaminants were identified in four colors and the corresponding samples were named red contaminant, yellow contaminant, gray contaminant and purple contaminant. According to the mining engineers these colors are present in all five varieties of ROM kaolin.



Figure 1. Kaolin ore containing lens with high concentration of red contaminant.

The samples were analyzed in the laboratory. Initially, under a binocular stereomicroscope to identify the structures, textures and mineral phases present. After, the mineralogy was identified with X-ray diffraction (XRD) and taking into account two analytical procedures, identified in this study as TOD (deposition) and TOC (calcination) procedures. In the TOD procedure the sample was pulverized and mounted on a sample holder; analyzed under  $2^\circ$  to  $70^\circ$  with  $2\theta$  CuK $\alpha$  radiation; a step of  $0.02^\circ$ ; a step time of 1 s. In the TOC procedure the sample was calcined at  $540^\circ\text{C}$  for 2 hours; mounted on a sample holder; analyzed under  $2^\circ$  to  $70^\circ$  with  $2\theta$  CuK $\alpha$  radiation; a step of  $0.02^\circ$ ; a step time of 1 s.

## RESULTS AND DISCUSSION

### *Red contaminants*

The red contaminants are minerals that occur in thin layers inside the ore. The structure of the red contaminant showed sedimentary layers of approximately one millimeter. In the associated material predominated the red color (subsample 1B). In some parts of the ore this material was cut by small venules of white (subsample 1A), purple (subsample 1C) and yellow (subsample 1D) material.

The diffractograms of the subsample 1A (Figure 2) show a blue line and a red line. These lines correspond respectively to the TOD and TOC procedures. Experimental measurements revealed that the primary peaks in the blue line correspond to kaolinite (Ka) and the secondary peaks to muscovite (Mu) and quartz (Qz). The TOC procedure emphasized the anatase peak (At) and confirmed muscovite and quartz by the resistance of these mineral phases in the calcination process. In subsample 1A no crystalline phase with iron was identified. The characteristics identified for the quartz were hyaline transparency, rounded forms for most grains and some grains with angular faces. The subsample 1A characteristics suggested intense leaching, which is probably related to the percolation of acidic solutions inside the sediments resulting from the decomposition of organic matter. These solutions probably acted on the remobilization of the iron containing compounds, altering the original color of the sediments.

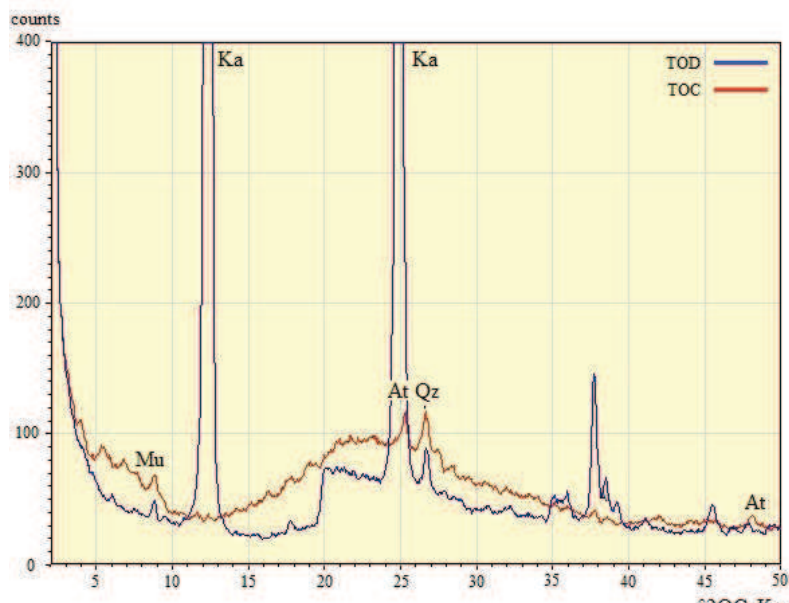


Figure 2. Diffractograms of subsample 1A XRD, white material.

The diffractogram of a subsample 1B (Figure 3), in the TOD procedure, revealed peaks of kaolinite (Ka), muscovite (Mu), goethite (Go) and hematite (Hm). In the TOC procedure, the goethite was eliminated and the peaks of hematite, muscovite and anatase (At) were highlighted. Quartz was not identified.

The diffractograms of subsample 1C (Figure 4), which corresponds to a material minority concentrated in a very thin layer, in the TOD procedure was emphasized the occurrence of kaolinite (Ka) and hematite (Hm) and subordinate muscovite (Mu) and quartz (Qz). Goethite either was not identified or its concentration is below the detection limit of the equipment. Therefore, the purple color was related to the presence of hematite. In the TOC procedure was confirmed the presence of anatase (At) and detrital muscovite.

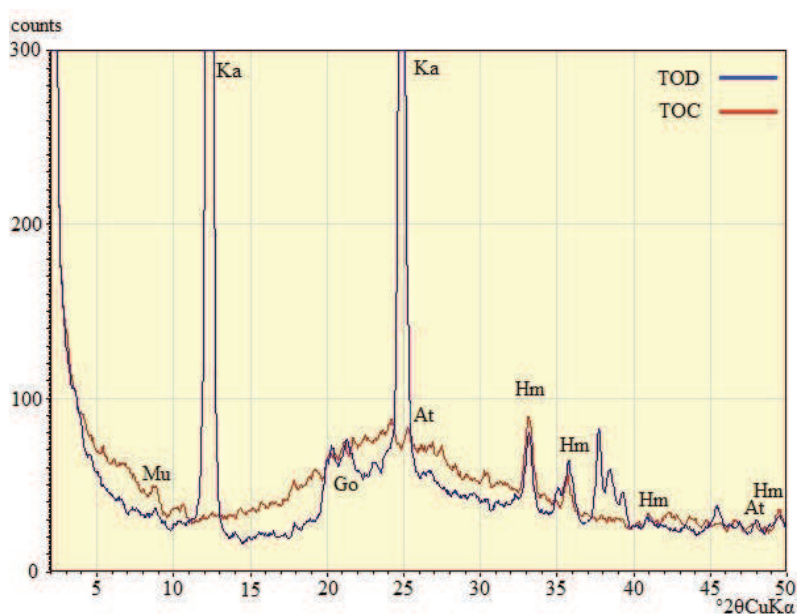


Figure 3. Diffractograms of subsample 1B XRD, red material.

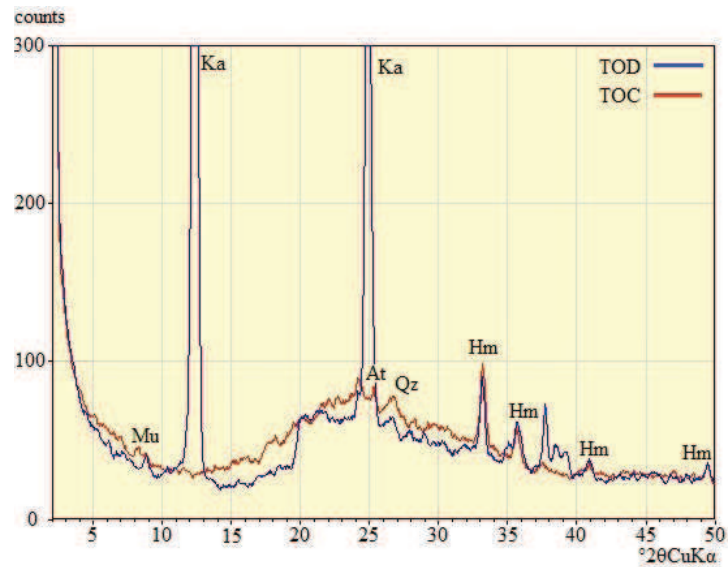


Figure 4. Diffractograms of subsample 1C XRD, purple material.

The diffractograms of subsample 1D (Figure 5), in the TOD procedure was emphasized the presence of kaolinite (Ka) and goethite (Go). The subsample 1D corresponds to the yellow material which occurred as spots forming thin films that are difficult to separate due to their small size. Muscovite (Mu) and quartz (Qz) occurred subordinately. Hematite was not identified. These characteristics seem to indicate that the yellow color is associated with the goethite. In the TOC procedure was revealed that goethite was unstable and easily transformed to hematite with heat.

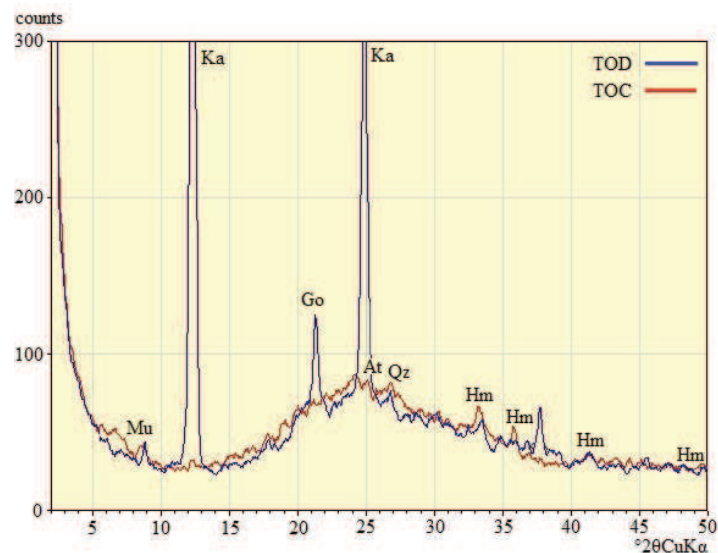


Figure 5. Diffractograms of subsample 1D XRD, yellow material.

The calcination of the subsamples 1A, 1B, 1C and 1D confirmed the presence of anatase. But this mineral phase occurred in high concentration only in subsample 1A, the white material, which contains higher concentrations of kaolinite. The other subsamples contained less anatase. This result indicated that

anatase tended to be present in the white material and, therefore, in the layers where the ore contained higher concentrations of kaolinite. As a consequence of this fact, the subsample 1D (yellow) presented very low concentrations of anatase.

According to Sabedot et al. (2011), chemical analysis performed in four samples showed similar titanium content, which can be interpreted as the effect of the material mixture during sample preparation, or may suggest that Ti was present in other phases of secondary minerals such as goethite. The latter is less plausible due to the geochemical properties of Ti, which has little mobility in a supergene environment and forms independent phases.

#### ***Yellow contaminant***

The yellow contaminant was associated with a yellow mass of friable texture consisting of sand and a few rounded clay fragments. The clay fragments (subsample 2A) were cohesive and up to five centimeters in diameter. The sandy material (subsample 2B) was formed by quartz grains mixed into a clay matrix that has yellow to clay color. The grains of quartz were well sorted, slightly rounded and greatly fractured. These characteristics indicate probable chemical changes in the medium after sedimentation. Inside the clay fragments were found quartz grains with much smaller sizes than those found in the sandy material. Some of these grains had silt dimensions.

Subsample 2A's XRD results of the TOD procedure showed a predominance of kaolinite and subordinate quartz and muscovite. These latter minerals were responsible for the white spots observed in binocular stereomicroscope. In the TOC procedure was confirmed the presence of muscovite and anatase, but no evidence of crystalline phases with iron were found. In the TOD procedure in subsample 2B, the predominance of quartz and subordinate kaolinite was confirmed, but no muscovite was identified as occurred in subsample 2A. In subsample 2B, the TOC procedure did not detect anatase. Again, this result confirmed the preferential positioning of anatase in the pelitic portion with higher concentrations of kaolinite.

#### ***Gray contaminant***

The material in which the gray color dominated, the grains were both cohesive and massive and the layers were structured in bands that showed several centimeters thick. The bands ranged in color from white to purple. Quartz was not easy to identify due the mineral occur as fine grains in clay fragments. The gray color was due to the interstratification of thin layers of light and dark colors, which was almost imperceptible. These layers were identified under a binocular stereomicroscope. Kaolinite predominated in the light layer (subsample 3A) and a mixture of kaolinite and a high concentration of black minerals (subsample 3B) constituted the dark layer.

Subsamples 3A and 3B showed similar results due to the difficulties in separating the light and dark layers under XRD analysis. According to the TOD procedure, both subsamples were predominantly kaolinite with subordinate muscovite. According to the TOC procedure, anatase, quartz and muscovite were identified, but hematite in either subsample was not identified. In this gray contaminant, the anatase again

appeared to be related to the predominant kaolinitic material.

### *Purple contaminant*

The purple material was composed of cohesive fragments with thin layers. Under a binocular stereomicroscope, these layers formed alternating material of different grain sizes. Probably, the thin-layered structure originated from sedimentation in which the coarse-grained layers were related to higher energy environments (quartz grains embedded in the clay matrix and forming fine sandstone). The thin-grained layers probably were deposited in environments with lower energy, basically forming a clay that showed no evidence of quartz under macroscopic analysis. In the present study the purple contaminant was divided into two subsamples, because the layers had different particle sizes. Subsample 4A containing a coarse granulometry with white mixed with purple. Subsample 4B containing smaller granulometry with purple color. Clay formed the main material.

The XRD results of the TOD procedure emphasized the presence of quartz and kaolinite in subsample 4A. In subsample 4B, kaolinite predominated and subordinate quartz, muscovite and hematite were also identified. The TOC procedure emphasized the presence of anatase and confirmed hematite and muscovite in both subsamples.

The relations of colors with mineral contaminants in the ore of the Ipixuna Mine are summarized in Table 1.

Table 1. Mineralogy associated with colors in subsamples of contaminating materials.

Contaminant	Subsample							
	A		B		C		D	
	Color	Mineral	Color	Mineral	Color	Mineral	Color	Mineral
Red	white	anatase	red	goethite	purple	hematite	yellow	goethite
		muscovite		hematite		muscovite		muscovite
Yellow	yellow (clay)	quartz	white (sand)	quartz		quartz		quartz
		anatase		anatase		anatase		
Gray	white	anatase	purple	anatase		anatase		anatase
		muscovite		muscovite		muscovite		
Purple	white	quartz	purple	hematite		hematite		hematite
		muscovite		muscovite		muscovite		
		anatase		anatase		anatase		anatase

All mineral contaminants formed sedimentary structures. The characteristics reported in the present study suggest that the Ipixuna Mine deposit evolved from a sequence of sedimentary rocks deposited in a relatively low energy environment. The distribution of iron minerals in the sediment profile was the main driver of color changes in the samples. The main mechanisms of iron mobilization were probably oxidation

and reduction processes, which may have been favored by the action of organic matter. The generating environment of the original sedimentary sequence was low-energy, in which mudstones predominated with thin layers of deposited siltstone and fine sandstone. The presence of rounded clay particles is an indicator of higher energy syngenetic events, in which the mudstone substrate was reworked.

## CONCLUSIONS

The Ipixuna Mine deposit contains different varieties of ROM kaolin that can be distinguished by the color of the ore. The colors depend on both the paragenesis and the concentration of mineral contaminants.

At several levels of the mine, small lenses with intense colors were identified, which indicate high concentrations of mineral contaminants mixed with the kaolinite. The contaminants were red, yellow, gray and purple.

The red contaminant was structured in millimeter-scaled layers of sedimentary origin, which was formed predominantly by kaolinite tinged with red color due to the intense presence of goethite and hematite. Sometimes this material was cut by millimeter-scaled veinlets of white material composed of kaolinite, muscovite, quartz and anatase. In the red contaminant were identified tiny purple layers composed mainly of hematite, muscovite and quartz, but without goethite and anatase. Subordinate to these, but also related to the red contaminant, were identified small patches of yellow color that indicate the presence of goethite. Hematite and anatase did not appear in this material.

The yellow contaminant was composed predominantly of kaolinite and secondarily of sandy material and rounded clay fragments. The sandy material was composed of quartz immersed in a yellow clay matrix. The rounded clay fragments were composed of quartz, muscovite and anatase. The yellow contaminant did not contain goethite and hematite.

The gray contaminant consisted of small interstratified layers of white and purple, which appeared gray in color to the naked eye. In these layers kaolinite was the main mineral with subordinate muscovite and quartz. The white material contained dispersed anatase. The purple layers contained high concentrations of anatase. Hematite and goethite were not detected in either layer.

The purple contaminant comprised interstratified layers with different particle sizes. The layers with coarser grain size were formed by quartz grains immersed in a clay matrix forming sandstone layers. The layers with finer particle sizes were formed by kaolinite and subordinate quartz, muscovite and hematite.

In all of the samples the anatase was found in the pelitic portion where kaolinite was the main mineral.

The colors, especially red, yellow and purple, were related to the mobilization of iron in the sediment profile, which was associated with oxidation and reduction processes.

## REFERENCES

- BLOODWORTH, A. J.; HIGHLEY, D. E.; MITCHELL, C. J. 1993. **Industrial minerals laboratory annual: kaolin**. United Kingdom: British Geological Survey. Technical Report WG/93/1, Mineralogy and Petrology Series. 80 p.
- CARNEIRO, B. S. et al. 2003. Caracterização mineralógica e geoquímica e estudo das transformações de fase do caulim duro da região do Rio Capim, Pará. **Cerâmica**, **49**:237-244.
- COSTA, M. L.; MORAES, E. L. 1998. Mineralogy, geochemistry and genesis of kaolins from the Amazon region. **Mineralium Deposita**, **33**(3):283-297.
- GÓES, A. M.; ROSSETTI, D. F.; MENDES, A. C. 2007. Heavy mineral as a tool to refine the stratigraphy of kaolin deposits in the Rio Capim area, northern Brazil. **Annals of the Brazilian Academy of Sciences**, **79**(3):457-471.
- GONÇALVES, I. G.; PETTER, C. O. 2007. Kubelka-Munk theory applied to industrial minerals: prediction of impurity content in kaolin. **REM-Revista Escola de Minas**, **60**(3):491-496.
- GONZÁLEZ, J. A.; RUIZ, M. C. 2006. Bleaching of kaolins and clay by chlorination of iron and titanium. **Applied Clay Science**, **33**:219-229.
- KOTSCHOUBEY, B.; DUARTE, A. L. S.; TRUCKENBRODT, W. 1999. Cobertura bauxítica e origem do caulim do Morro do Felipe, baixo Rio Jari, estado do Amapá. **Revista Brasileira de Geociências**, **29**(3):331-338.
- MONTES, C. R. et al. 2002. Genesis, mineralogy and geochemistry of kaolin deposits of the Jari River, Amapá State, Brazil. **Clay and Clay Minerals**, **50**(4):494-503.
- MURRAY, H. H. 2000. Traditional and new applications for kaolin, smectite and palygorskite: a general overview. **Applied Clay Science**, **17**:207-221.
- MURRAY, H. H.; ALVES, C. A.; BASTOS, C. H. 2007. Mining, processing and applications of the Capim Basin kaolin, Brazil. **Clay Minerals**, **42**(2):145-151.
- MURRAY, H. H.; PARTRIDGE, P. 1981. Genesis of Rio Jari kaolin. In: INTERNATIONAL CLAY CONFERENCE, 1981, Elsevier, Amsterdam, p. 279-281.
- RAGHAVAN, P. 2010. Technology development for kaolin processing. In: XI INTERNATIONAL SEMINAR ON MINERAL PROCESSING TECHNOLOGY (MPT-2010), NML Jamshedpur, India, p. 683-690.
- RAITANI, R. et al. 2012. Chemically enhanced magnetic separation technologies for kaolin processing. **Minerals & Metallurgical Processing**, **29**(1):20-26.
- RIBEIRO, F. R. et al. 2003. Identification of iron-bearing minerals in solid residues from industrial kaolin processing. **Hyperfine Interactions**, **148-149**(1-4):47-52.
- SABEDOT, S.; PETTER, C. O.; SAMPAIO, C. H. 2011. Espectrocolorimetria de variedades de caulim da jazida Ipixuna, no estado do Pará. **REM-Revista Escola Minas**, **64**(3):363-368.
- SCHULZ JR., A. 2000. **Kaolin Exploration in the Capim River region, state of Pará**. CPRM, Informe de Recursos Minerais, Série Oportunidades Minerais, n. 23. 20 p.
- SENA, G. L. S.; MÁRTIRES, R. A. C. 2011. **Caulim**. Sumário Mineral. Departamento Nacional de Produção Mineral, Brasília, Brasil. Disponível em <<http://www.dnpm.gov.br/dnpm/sumarios/sumario-mineral-2011>>. Acesso em 12 jun 2015.
- SOUSA, D. J. L.; VARALÃO, A. F. D. C.; YVON, J. 2006. Geochemical evolution of the Capim River kaolin, northern Brazil. **Journal of Geochemical Exploration**, **88**:329-331.
- STYRIAKOVÁ, I.; STYRIAK, I. 2000. Iron removal from kaolins by bacterial leaching. **Ceramics**, **44**(4):135-141.
- VARELA, J. J. et al. 2005. Controle de qualidade no processamento de polpas de caulim utilizando propriedades óticas. **REM-Revista Escola de Minas**, **58**(3):201-206.

WILSON, I. R.; SANTOS, H. S.; SANTOS, P. S. 1998. Caulins brasileiros: alguns aspectos da geologia e da mineralogia. *Cerâmica*, **44**:118-129.

WILSON, I. R.; SOUZA-SANTOS, H.; SOUZA-SANTOS, P. 2006. Kaolin and halloysite deposits of Brazil. *Clay Minerals*, **41**:697-716.

YANIC, G. 2011. Mineralogical, crystallographic and technological characteristics of Yaylauolu kaolin (Kütahya, Turkey). *Clay Minerals*, **46**(3):397-410.